Systems and Control Group

Thesis Systems and Control

Optimization of the downstream processing of microalgal biomass to biodiesel

B. J. Koetzier

June 2012

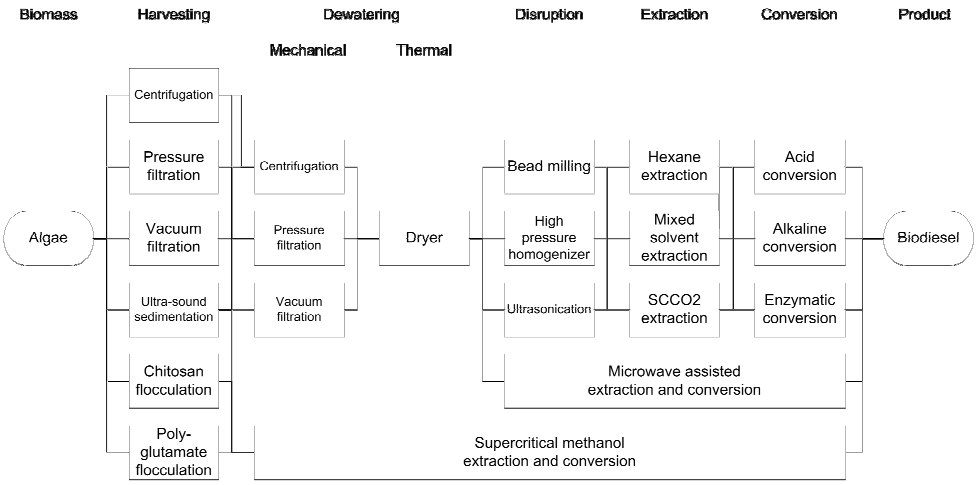

WAGENINGEN UNIVERSITY
AGROTECHNOLOGY AND
FOOD SCIENCES

WAGENINGEN UR

Optimization of the downstream processing of microalgal biomass to biodiesel

Name course	:	Thesis project Systems and Control
Number	:	SCO-80436
Study load	:	36 ects
Date	:	June 2012

Student	:	B. J. Koetzier
Registration number	:	88-06-16-454-120
Study programme	:	MBT (Biotechnology)
Supervisor(s)	:	Dr.ir. A.J.B. van Boxtel Ir. P. M. Slegers
Examiners	:	dr.ir. K.J. Keesman,
Group	:	Systems and Control Group
Address	:	Bornse Weilanden 9 6708 WG Wageningen the Netherlands Tel: +31 (317) 48 21 24

Abstract

Producing biodiesel from microalgae is one way to provide the world with a renewable energy source. Unfortunately not much is known about the energy requirement for different methods of downstream processing of microalgal biomass into biodiesel, and how to reduce the energy requirements.

In this project five process steps for downstream processing are considered: harvesting, dewatering, disruption, extraction and transesterification. For each step a number of possible unit operations are modelled using mass and energy balances. With these models the energy consumption of several combinations of processing units in downstream processing is calculated.

To search for the best combinations of unit operations in the process chain, two techniques are used. The first technique is binary simulation. Here processes are considered at specific operating conditions. The best combination of unit operations is then found by calculating every possible route. Calculating all the routes also gives extra information, which can be used to compare different process choices. The second technique uses an advanced optimization technique, which considers also flexibility in the operating conditions. The results show that the best process routes for both cases are those that convert wet algae to biodiesel. This removes the need for extensive dewatering steps. These routes also combine disruption, extraction and transesterification into one unit operation, which further reduce the energy requirement. When the results of the binary simulations and the advanced optimization are compared, it is shown that the advanced optimization gives improvements from 10% to 40% in energy uptake.

Table of contents

1. Introduction

1.1 Background

In recent years crude oil reserves have been steadily declining. At the same time yearly oil demand has increased due to industrial growth in emerging economies third world countries. To resolve this problem the scientific and industrial communities have been searching for alternative energy resources. While there are numerous options, all of them have drawbacks. This can be in the total energy production, the sustainability of the process, waste management or any of a number of other limitations. One of the promising options is the production of biodiesel from microalgal biomass.

The most important feature of microalgae is the ability to fix carbon dioxide in organic compounds using solar energy. These organic compounds are then used for biomass assimilation. Under certain conditions, for instance nitrogen deprivation, microalgae are not able to produce biomass. Instead, they store the energy in triacyl-glycerides. After extracting triacyl-glycerides from the biomass, they can be converted to biodiesel by a transesterification with short alcohols, such as methanol.

The production process of biodiesel from microalgae consists of the following processing steps: cultivation, harvesting, dewatering, disruption, extraction, conversion and waste disposal. Unfortunately, a number of these steps have a high demand for energy and materials. This leads to a low net energy return. To date there is no microalgal biofuel system that has achieved economic viability (Stephens *et al*, 2010). A number of options have been suggested to improve this situation. An example is the anaerobic digestion of the residual biomass. This process produces methane from the waste biomass (Sialve *et al*, 2009). The methane can be used as an energy source in production of biodiesel (for example drying of algal biomass) or used as an energy source for other applications

A major part of the energy and materials are consumed during downstream processing of the microalgal biomass. Brentner et a, 2011l, described a process chain which can be considered as a base case for biodiesel production from microalgae. It uses techniques that are used in

similar processes on an industrial scale: centrifugation; drying; drill pressing; hexane extraction, transesterification with methanol (Brentner *et al*, 2011). This process has a number of bottlenecks. The biggest bottleneck is the separation of the algae from the cultivation broth, because the suspension has a low mass fraction of cells (Amaro *et al*, 2011). This means that large volumes have to be processed for small amounts of biomass, which leads to a low energy efficiency. But there are also bottlenecks in the efficient disruption of algae due to their cell wall. For a number of processes a drying step is required. If this step could be removed the energy consumption would go down.

Since these processes are not fully optimized yet, alternatives and how they interact with each other have to be considered. Therefore a good combination of downstream processing steps needs to be found, so that we can further reduce the demand for energy and materials.

1.2 Problem definition

The main problem is summarized by the following question:

> What is the best combination of unit operations in respect to the material and energy requirements for the downstream processing of microalgal biomass to biodiesel?

Here the focus will lie first on the energy consumption and then on the material use. The eventual purpose is to find the best combination of process steps using different optimization routines.

In the first part of this project potential unit operations for each process step are modelled. Mass and energy balances describe the relationships between the properties of the entering and leaving streams. For key variables, like the microalgal recovery and concentration factors, relationships are taken from the literature. The energy consumption depends largely on the volumetric flow rate entering the unit operation. And the recovery factor depends heavily on the material use. Therefore extra attention is given to the biomass reduction in each unit operation. From the energy balances the power consumption for each process option is calculated. This information is combined with the results from the mass balances to find energy use per kilogram of biomass. To improve the energy efficiency of the process chain, attention is given to the formation of by-products and the recovery of reagents.

In the second part of this project the possibilities are investigated to optimize the whole downstream processing. The optimization searched for the best product routing through all possible combination of unit operations.. The goal is to reduce the energy and material demands. These include flocculants, solvents and reactants. First a binary optimization is used. This type of optimization keeps all the process parameters constant. Constraints are put on this system, so that only possible process routes will be considered. For example a conversion step cannot occur before an extraction step. The optimization procedure evaluates the different options for each process step and returns the best combination of the possible processes. This kind of optimization has been done before (Brentner *et al*, 2011).

Another area of interest is the flexibility of the unit operations. A number of studies have been done that look at different process chains. These studies mostly concern cases, where the process parameters are kept constant during the optimization. This excludes many solutions, which might be very energy efficient. To gather these insights a second optimization is carried out. This optimization includes the search for the best product routing (like in the binary optimization) and optimizes simultaneously the values of its process parameters. Using mixed integer non-linear programming constraints are put on the system. These include the same constraints as the binary optimization, but also constraints on the process parameters. Thus these parameters will be flexible within their bounds. The optimization will return the best process chain. This solution should be an improvement over the solution from the binary optimization.

2. Model description

For downstream processing of microalgae to biodiesel six functional steps are considered: harvesting, dewatering, disruption, extraction, conversion and waste disposal. For each of these steps several unit operations are possible (see Fig. 2.1). For all unit operations in figure 2.1 a basic input-ourput model was made to relate the flows out of the system to the flows into the system through the use of mass and energy balances for each of these processes. The general form of these balances is

$$\frac{dX}{dt} = \sum_{i=1}^{m} F_i * C_{X,i} - \sum_{j=1}^{n} F_j * C_{X,j} = 0 \qquad \text{Eq. 2.1}$$

$$\frac{dE}{dt} = \sum_{i=1}^{m} F_i * E_i - \sum_{j=1}^{n} F_j * E_j = 0 \qquad \text{Eq. 2.2}$$

There is no accumulation of mass or energy, therefore equations 2.1 and 2.2 are equal to zero Where *dX/dt* is the accumulation of compound X (kg h^{-1}), *dE/dt* is the accumulation of energy (J h^{-1}), *F* is the flow rate (m^3 h^{-1}), C_x is the concentration of component X (kg m^{-3}) and *E* is the energy content (J m^{-3}). The flows in and out of the system are described by the subscripts *i=1..m* and *j=1..n* respectively.

Matlab functions were created for these balance equations to perform the calculations. An example is given in Appendix A. All processes are assumed to scale linearly and a relationship for one algae species holds for every algae species. This means that all processes that have been considered on laboratory and pilot scale, will work the same on commercial scale. The oil content of microalgae is taken to be 30% (Demirbas *et al*, 2010). The heat capacity of the algae slurry is assumed to be the same as the heat capacity of water. It is assumed that in harvesting, dewatering and disruption processes no operating energy is transferred to the algae slurry.

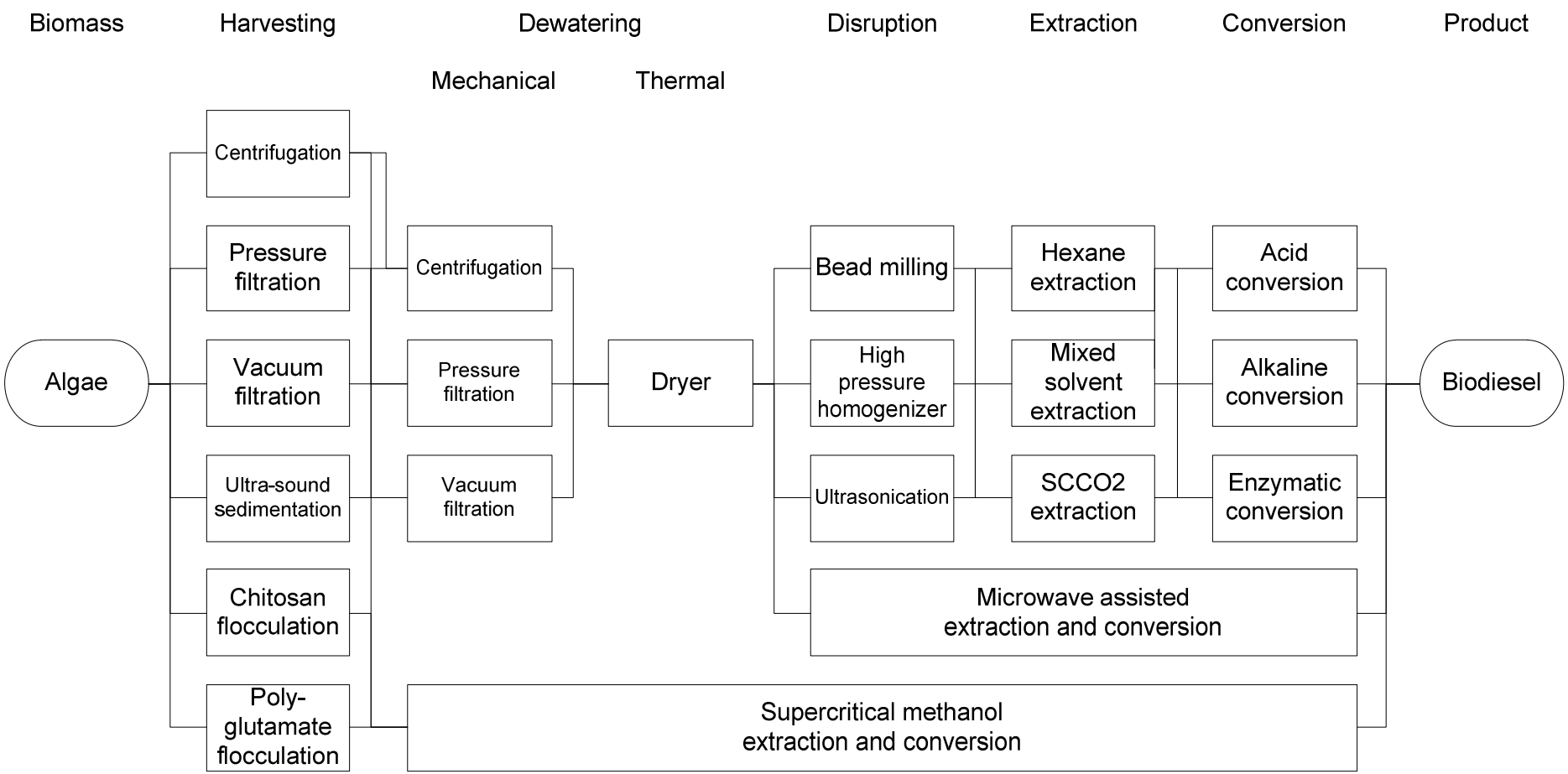

Fig. 2.1 – Superstructure of all possible routings along the unit operations in each step in the downstream processing of microalgae to biodiesel. Included are harvesting, dewatering, disruption, extraction and conversion. Unit operations are described by squares, the start and end by ovals and the lines describe the possible combinations of process steps.

2.1 Harvesting

During harvesting microalgae are separated from the cultivation broth. The two types of harvesting processes considered are shown in Figure 2.2. In the first type of process only energy to separate the algae from the fermentation broth is used (see figure 2.2a). This so-called “mechanical harvesting” includes centrifugation, vacuum filtration, pressure filtration and ultra-sound-sedimentation. The second type is flocculation and here energy is used to mix the microalgae with a flocculant, after which the algae are left for precipitatation . Both types of harvesting are described by the following mass balance:

$$0 = F_{A,in} * \ C_{A,in} - F_{A,out} * C_{A,out} - F_{A,byprod} * C_{A,waste} \quad \text{Eq. 2.3}$$

$$C_{A,out} = C_{A,in} * Cf \quad \text{Eq. 2.4}$$

$$F_{A,out} = \frac{F_{A,in} * C_{A,in} * R}{C_{A,out}} \quad \text{Eq. 2.5}$$

$$F_{A,waste} = F_{A,in} - F_{A,out} \quad \text{Eq. 2.6}$$

$$C_{A,waste} = \frac{F_{A,in} * C_{A,in} * (1 - R)}{F_{A,waste}} \quad \text{Eq. 2.7}$$

Where F is the volumetric flow rate ($m^3\ s^{-1}$), C is the concentration ($kg\ m^{-3}$), R is the microalgae recovery (wt/wt) and Cf is the concentration factor (-). The subscript A and F are algae and flocculant respectively.

The energy balance for the first type of harvesting is given by:

$$0 = c_p * F_{A,in} * \rho_A * T_{in} - c_p * F_{A,out} * \rho_A * T_{out} - c_p * F_{A,waste} * \rho_W * T_{out} \quad \text{Eq. 2.8}$$

Where F is the volumetric flow rate ($m^3\ s^{-1}$), T is the temperature (K), H is power requirement ($J\ s^{-1}$), ρ is the density ($kg\ m^{-3}$) and c_p is the heat capacity ($J\ kg^{-1}\ K^{-1}$). The subscripts A and W denote algae and water respectively.

The energy balance for the second type of processes (flocculation) is given in 2.2.2.

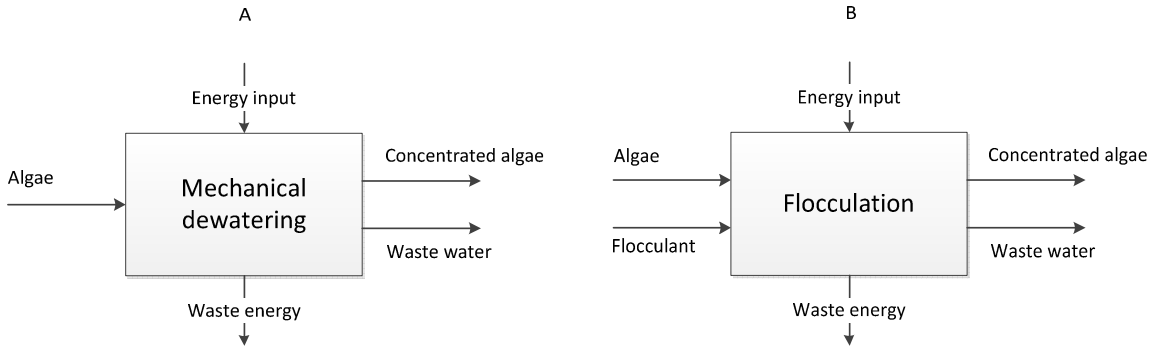

Fig. 2.2 – figure 2.2a describes the harvesting of microalgae using only energy. Figure 2.2b describes the harvesting of algae using a flocculant and energy.

2.2.1 Mechanical harvesting

Wileman *et al* describes three processes of mechanical harvesting, centrifugation, pressure filtration and vacuum filtration (Wileman *et al*, 2012). In centrifugation cells are separated by a difference in density. In both filtration steps separation is based on particle size. The difference between these two filtration methods is that in pressure filtration the pressure difference is created by a pressure on the retentate side, while in vacuum filtration the pressure difference is created by a vacuum on the filtrate side. Brentner *et al* used a microalgae recovery of 95 % for these processes (Brentner *et al*, 2011). The concentration factor is the decision variable in these processes.

According to Wileman *et al* the energy consumption is:

$$H = E * F_{A,in} * Cf \qquad \text{Eq. 2.9}$$

Where H is the energy consumption (J s^{-1}), E is the energy requirement for each process (J m^{-3}), F is the volumetric flow rate (m^3 s^{-1}) and Cf is the concentration factor (-).
The energy requirements are given in table 2.1

Table 2.1 – Energy requirement for each process (Wileman *et al* 2012).

Process	**Energy requirement (J m^{-3} of inflow)**
Centrifugation	11880000
Pressure filtration	1692000
Vacuum filtration	7245000

Bosma *et al* describes a process to separate algae using ultra-sound sedimentation to separate algae. First the algae slurry is pumped into a reactor vessel. Second, ultra-sound is used to create a standing wave in the reactor, which creates areas of low potential energy in the nodes of the standing wave and areas of high potential energy in the bellies of the standing wave. As a result the microalgae migrate to the areas of low potential energy (see Fig 2.3). When the standing wave is removed, the flocks sediment on the bottom of the vessel and can be recovered.

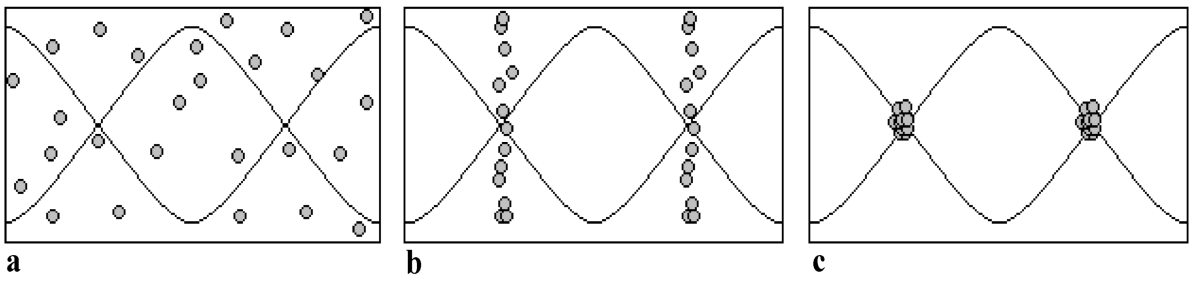

Fig. 2.3 – Harvesting of microalgae by ultra-sound sedimentation. Image taken from Bosma *et al*, 2003.

The recovery and concentration factor depend on biomass concentration, flow rate, time frequency, power input and ratio between F_{out} and F_{in}. Bosma *et al* estimate the coefficients for these variables using a response surface methodology (RSM), which results in the following two polynomials:

$$R = a0 + a1 * C_{A,in} + b1 * F_{A,in} + c1 * t + d1 * H + b2 * F_{A,in}^2 + b3 * t^2 + ab * C_{A,in} * F_{A,in} + ad * C_{A,in} * H + bd * F_{A,in} * H \quad \text{Eq. 2.10}$$

$$Cf = a0 + a1 * C_{A,in} + b1 * F_{A,in} + e1 * \frac{F_{A,out}}{F_{A,in}} + b2 * F_{A,in}^2 + ae * C_{A,in} * \frac{F_{A,out}}{F_{A,in}} \quad \text{Eq. 2.11}$$

See supplement 1 USSed.m for the constants for both equations.

2.2.2 Flocculation

In flocculation processes energy is used to mix a flocculant and algae to force them to coagulate (see Fig 2.2b). The microalgae flocks are left to sediment. The flocculant improves the sedimentation properties of the algae-complex compared to untreated algae. Both chitosan flocculation and poly-glutamate flocculation adhere to this principle. In both cases the microalgal recovery depends on biomass and flocculant concentration. The flocculant

concentration in the product stream is very low and therefore neglected. As a result the mass balance is the same as for the other harvesting processes. The decision variable is the chitosan concentration.

The energy balance for flocculation is an expansion of the energy balance given in section 2.2.1.

$$0 = c_p * F_{A,in} * \rho_A * T_{A,in} + c_p * F_{F,in} * \rho_W * T_{F,in} + H - c_p * F_{A,out} * \rho_A * T_{out} - c_p * F_{A,waste} * \rho_W * T_{out} \quad \text{Eq. 2.12}$$

Where F is the volumetric flow rate ($m^3\ s^{-1}$), T is the temperature (K), H is the power consumption ($J\ s^{-1}$), ρ is the density ($kg\ m^{-3}$) and c_p is the heat capacity ($J\ kg^{-1}\ K^{-1}$). The subscripts *A*, *F* and *W* denote algae, flocculant and water respectively.

The power consumption is given by:

$$H = E * \left(F_{A,in} + F_{F,in}\right) \quad \text{Eq. 2.13}$$

Where H is the energy requirement ($J\ s^{-1}$), E is the specific energy requirement ($J\ m^{-3}$) and F is the volumetric flow rate ($m^3\ s^{-1}$).
Brentner *et al* estimate that the energy requirement for chitosan flocculation is 360 $J\ m^{-3}$. Since both flocculation processes have large similarities, it is assumed that the same value holds for the poly-glutamate flocculation.

Chitosan flocculation has been described by Morales *et al* (Morales *et al*, 1985). Flocculation efficiency was evaluated by mixing microalgae with different amounts of chitosan. A hyperbolic tangent function was fitted to this data to produce an equation for the flocculation efficiency (see supplement 2 flocfit.m).

$$R = 1 * \tanh(\ 59.21 * C_{F,in}) \quad \text{Eq. 2.14}$$

This equation holds for one biomass concentration. Biomass concentration and chitosan concentration scale linearly (Tenney *et al*, 1969), so the flocculation efficiency is given by:

$$R = 1 * \tanh(59.21 * \frac{C_F * C_{A,ref}}{C_A}) \quad \text{Eq. 2.15}$$

Where *R* is the microalgal recovery (kg kg^{-1}) and *C* is the biomass concentration (kg m^{-3}). The subscripts F, A and ref stand for flocculant, algae and reference respectively.
The concentration factor is calculated by:

$$Cf = \frac{C_{A,out}}{C_{A,in}} \quad \text{Eq. 2.16}$$

Where *Cf* is the concentration factor (-) and C_A is the biomass concentration (kg m^{-3}).
For this flocculation method the final concentration is assumed to be 5%.

In the second type of flocculation that has been considered, microalgae are flocculated with poly-glutamate (Hongli *et al*, 2012). The microalgal recovery and concentration factor are affected by biomass concentration, poly-glutamate concentration and salinity (Hongli *et al*, 2012) and are described by one polynomial each:

$$R = 0.01 * (a0 + a1 * C_F + b1 * C_A + c1 * C_{salt} + a2 * C_F^2 + b2 * C_A^2 + c2 * C_{salt}^2 + ab * C_F * C_A + ac * C_F * C_{salt} + bc * C_A * C_{salt}) \quad \text{Eq. 2.17}$$

$$Cf = a0 + a1 * C_F + b1 * C_A + c1 * C_{salt} + a2 * C_F^2 + b2 * C_A^2 + c2 * C_{salt}^2 + ab * C_F * C_A + ac * C_F * C_{salt} + bc * C_A * C_{salt} \quad \text{Eq. 2.18}$$

Where *R* is the microalgal recovery (kg kg^{-1}), *Cf* is the concentration factor (-) and *C* is the concentration (kg m^{-3}). The values for the constants are given in table A.2 (see appendix A). See supplement 3 GFloc.m for the constants for both equations.

2.2 Dewatering

Algae biomass/algae slurry is further concentrated by mechanical and thermal dewatering. The algae stream entering the dewatering system will produce a concentrated product stream and a waste stream that contains water and a small amount of algae (see Fig 2.5). For mechanical drying a force is used to separate the cells, while heat is used for thermal drying. The unit operations considered for mechanical dewatering are centrifugation, vacuum filtration and pressure filtration. Section 2.1.1 gives the details of these processes.

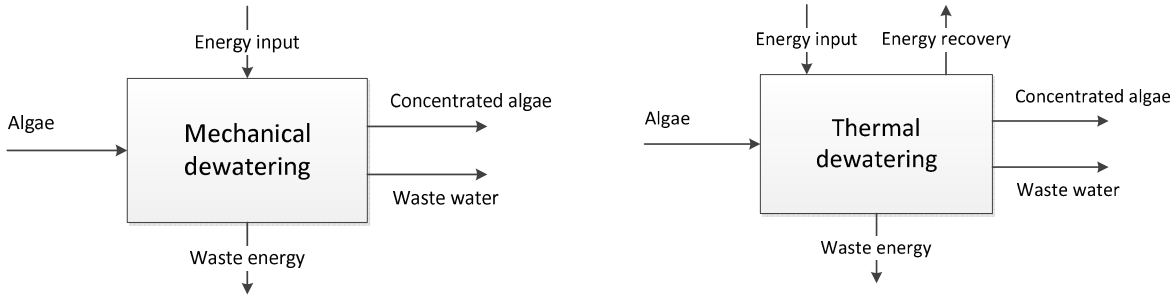

Fig. 2.4 – Dewatering of microalgae to concentrate them further.

2.2.1 Thermal dewatering

In thermal drying heat is used to evaporate water from the algal slurry. The concentration factor is the decision variable. The mass balance for thermal drying is given by:

$$0 = F_{A,in} * C_{A,in} - F_{A,out} * C_{A,out} - F_W * \rho_W \quad \text{Eq. 2.19}$$

$$C_{A,out} = C_{A,in} * Cf \quad \text{Eq. 2.20}$$

$$F_{A,out} = F_{A,in} * \frac{C_{A,in}}{C_{A,out}} \quad \text{Eq. 2.21}$$

$$F_W = (F_{A,in} * C_{A,in} - F_{A,out} * C_{A,out})/(\rho_W) \quad \text{Eq. 2.22}$$

Where F is the volumetric flow rate ($m^3\ s^{-1}$), C is the concentration (kg m^{-3}), Cf is the concentration factor and ρ is the density (kg m^{-3}). The subscripts A and W stand for algae and water respectively.

The energy balance for thermal drying is:

$$0 = c_p * F_{A,in} * \rho_A * T_{in} + H * \eta - c_p * F_{A,out} * \rho_A * T_{out} - F_W * \rho_W * \Delta H_{vap} \quad \text{Eq. 2.23}$$

Where F is the volumetric flow rate ($m^3\ s^{-1}$), ρ is the density ($kg\ m^{-3}$), T is the temperature (K), c_p is the heat capacity ($J\ kg^{-1}\ K^{-1}$), H is the power consumption ($J\ s^{-1}$), η is the efficiency of the heater (-) and ΔH_{vap} is the heat of evaporation ($J\ m^{-3}$).
The efficiency of the heater is assumed to be 0.5 (Devki Energy Consultancy)

2.3 Disruption

For many extraction processes cells have to be disrupted first. In the options considered, this disruption is accomplished by subjecting a stream of microalgae to a force which destroys the cell structure (see Fig 2.3).

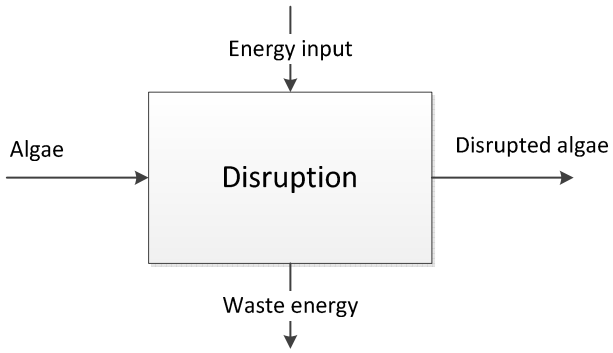

Fig. 2.5 – Schematic of the disruption of microalgae.

During the disruption of microalgae the biomass concentration in the water phase stays constant. Instead a certain amount of cells are disrupted releasing the lipids that are inside.
Therefore the mass balance relates the released lipids to the lipid content of the microalgae.
The algal oil content is assumed to be 30% (Amaro *et al*, 2011). After disruption the out flow contains intact and disrupted algae with lipids inside. Only from the disrupted algae can the lipids be extracted.
The mass balance is given by:

$$0 = F_A * C_{L,in} - F_A * C_{L,out} - F_A * C_{L,waste} \quad \text{Eq. 2.24}$$
$$C_{L,in} = C_{A,in} * AOC \quad \text{Eq. 2.25}$$
$$C_{L,out} = C_{A,in} * D * AOC \quad \text{Eq. 2.26}$$
$$C_{L,waste} = C_{A,in} * (1 - D) * AOC \quad \text{Eq. 2.27}$$

Where F is the volumetric flow rate ($m^3\ s^{-1}$), C is the concentration ($kg\ m^{-3}$), AOC is the algal oil content (wt%) and D is the disruption efficiency (wt/wt). The subscripts A and L are algae and lipids respectively.

The energy balance is given by the following equation:

$$0 = c_p * F_A * \rho_A * T_{in} - c_p * F_A * \rho_A * T_{out} \quad \text{Eq. 2.28}$$

2.3.1 Bead milling

For bead milling the microalgae slurry is mixed with beads, followed by agitation. As a result the cellular structure of the algae disintegrates. The degree of disruption is influenced by the biomass concentration, flow rate, beads filling, speed of agitator and bead diameter. Doucha *et al* described a power function relating the degree of disruption to these process parameters (Doucha *et al*, 2008).

$$D = a0 * F_{A,in}^{n1} * d_b^{n2} * C_{beads}^{n3} * v^{n4} * C_{A,in}^{n5} \quad \text{Eq. 2.29}$$

Where F is the volumetric flow rate ($m^3\ s^{-1}$), d is the diameter of the beads, C_{beads} is the percentage of the chamber that is filled with beads (%), v is the rotation speed ($m\ s^{-1}$) and C_A is the algae concentration ($kg\ m^{-3}$). See supplement 3 BM.m for the constants.

The energy consumption is 3.3 kW (Doucha *et al*, 2008)

2.3.2 High pressure homogenizer

In a high pressure homogenizer the algae slurry is forced through a valve at high pressure. The sheer stress disintegrates the microalgae cells. 73% of the algae are disrupted at 850 bar (Halim *et al*, 2012). The power consumption is given by:

$$H = p * F_{A,in} \quad \text{Eq. 2.30}$$

Where H is the energy requirement ($J\ s^{-1}$), p is the pressure ($N\ m^{-2}$) and F is the volumetric flow rate ($m^3\ s^{-1}$).

2.4.3 Sulphuric acid treatment

Sulphuric acid treatment disrupts cells by adding a strong acid to the microalgae slurry. According to Halim *et al* the degree of disruption is 30% at 160 degree Celsius. The energy consumption can be derived from Eq. 2.28).

2.4 Extraction

In an extraction procedure the slurry with disrupted algae are mixed with a solvent. Lipids transfer from the water phase to the solvent phase, because of a difference in the solubility in the water phase and solvent phase (see Fig 2.6). The mass balance to describe extraction is:

$$0 = F_A * C_{L,in} - F_A * C_{L,waste} - F_S * C_{L_{out}} \quad \text{Eq. 2.31}$$

$$C_{L,out} = \frac{F_A * C_{L,in} * Y}{F_H} \quad \text{Eq. 2.32}$$

$$C_{L,waste} = \frac{F_A * C_{L,in} * (1 - Y)}{F_H} \quad \text{Eq. 2.33}$$

Where F is the volumetric flow rate ($m^3\ s^{-1}$), C_L is the lipid concentration ($kg\ m^{-3}$), AOC is the algal oil content ($kg\ kg^{-1}$) and Y is the fraction of the lipids that is extracted ($kg\ kg^{1}$). The lipid yield is an important variable to calculate and it depends on the process parameters. When heating is used 50% of the energy input can be recovered.

The energy balance is given by:

$$0 = c_{p,A} * F_A * \rho_A * T_{A,in} + c_{p,S} * F_S * \rho_S * T_{S,in} + H - c_{p,A} * F_{A,out} * \rho_A * T_{out} - c_{p,S} * F_S * \rho_S * T_{out} \quad \text{Eq. 2.34}$$

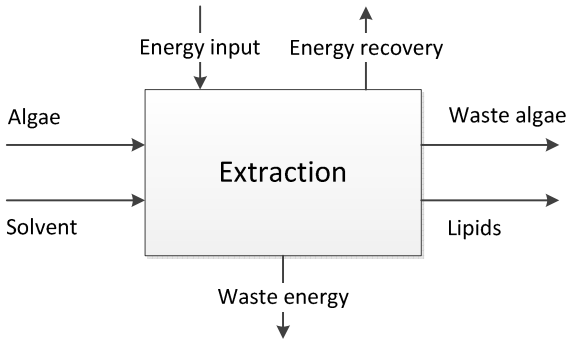

Fig. 2.6 – Extraction of lipids from disrupted microalgae.

2.4.1 Organic solvent extraction

Two organic solvent extractions are considered. The first is a n-hexane extraction, the second is a mixed solvent extraction. The lipid yield (g extracted lipid / g total lipid) at specific temperature is given in Table 2.2.

Table 2.2 – Extraction yield for n-hexane and mixed solvent extractions at a specific temperature.

Extraction	**Temperature (°C)**	**Extraction yield (%)**
n-hexane	20	95
Mixed solvent	50	91

2.4.2 Supercritical CO_2 extraction

In a supercritical carbon dioxide extraction the lipids are extracted from the microalgae using carbon dioxide. A mixture of hexane and methanol is added to carbon dioxide as modifier. Adding the modifier modifies the extraction properties of carbon dioxide. Char *et al* described the extraction yield as a function of the temperature, pressure and the ratio between hexane and methanol (Char *et al*, 2011):

$$Y = a0 + a1 * T + b1 * p + c1 * r + a2 * T^2 + b2 * p^2 + c2 * r^2 + ab * T * p + ac * T * r + bc * p * r \quad \text{Eq. 2.35}$$

Where Y is the lipid yield (kg kg^{-1}) , T is the temperature (°C), p is the pressure (bar) and r is the ratio between hexane and methanol. See supplement 4 SCCO2.m for the values of the constants.

The energy balance for supercritical carbon dioxide extraction has an expansion for the energy consumption compared to the other extractions.

$$H = H_T + F_{L,in} * p \quad \text{Eq. 2.36}$$

Where $H$is the energy consumption (J s^{-1}), H_T is the energy consumption for heating (J s^{-1}) as in Eq. 2.35, F is the volumetric flow rate (m^3 s^{-1}) and p is the pressure (N m^{-2})

2.5 Transesterification

During conversion from lipids to biodiesel the ester bonds in triacyl glycerides are broken. The free fatty acids, produced in this reaction, react with methanol to form fatty acid methyl esters(FAME) (see Fig 2.7). The process is described by three mass balances, one for lipids, one for FAME's and one for methanol.

$$0 = F_L * C_{L,in} - F_L * C_{L,out} - L \quad \text{Eq. 2.37}$$

$$0 = L - F_L * C_{F,out} \quad \text{Eq. 2.38}$$

$$0 = F_{M,in} - F_{M,out} - M \quad \text{Eq. 2.39}$$

$$L = F_L * C_{L,in} * Y \quad \text{Eq. 2.40}$$

$$C_{F,out} = \frac{L}{F_L} \quad \text{Eq. 2.41}$$

$$C_{L,out} = \frac{F_A * C_{L,in} - L}{F_L} \quad \text{Eq. 2.42}$$

$$M = 3 * \frac{L}{m_L} * m_M * \frac{1}{\rho_M} \quad \text{Eq. 2.43}$$

$$F_{M,out} = F_{M,in} - M \quad \text{Eq. 2.44}$$

Where F is the volumetric flow rate ($m^3\ s^{-1}$), C is the concentration ($kg\ m^{-3}$), L is the lipid conversion ($kg\ s^{-1}$), M is the methanol consumption ($kg\ s^{-1}$), m is the molecular weight ($kg\ mol^{-1}$) and ρ is the density ($kg\ m^{-3}$). The subscripts L, F and M are lipid, FAME and methanol respectively.

The energy balance for transesterification is described by:

$$0 = c_{p,L} * F_L * \rho_L * T_{L,in} + c_{p,M} * F_M * \rho_M * T_{M,in} + H - c_{p,F} * F_{F,out} * \rho_F * T_{out} - c_{p,M} * F_M * \rho_M * T_{out} \quad \text{Eq. 2.45}$$

Where c_p is the heat capacity ($J\ kg^{-1}\ K^{-1}$), T is the temperature (K) and H is the power consumption ($J\ s^{-1}$).

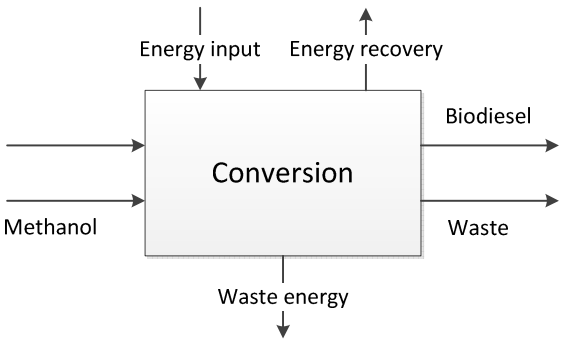

Fig. 2.7 – Conversion of extracted lipids to FAME's.

2.5.1 Acid catalysed transesterification

In this process the transesterification is catalysed by hydrochloric acid. At 70°C 98% of the lipids are converted to FAME's (Brentner *et al*, 2011)

2.5.2 Alkaline catalysed transesterification

In the alkaline transesterification the process is catalysed by a base. Rashid *et al* described this process for rice bran oil. Since the composition of this oil is similar to the oil from microalgae, it is assumed that this process gives an accurate description for the conversion yield for microalgae lipids.

The lipid yield is described as a function of the molar ratio between methanol and lipids, the catalyst concentration (%), the temperature (°C) and the reaction time (min):

$$Y = a0 + a1 * r + b1 * c + c1 * T + d1 * t + a2 * r^2 + b2 * c^2 + c2 * T^2 + d2 * t^2 + ab * r * c + ac * r * T + ad * r * t + bc * C * T + bd * c * t + cd * T * t \quad \text{Eq. 2.46}$$

Where *r* is the molar ration between methanol and algae (wt/vol), *T* is the temperature (°C) and t is the reaction time (min). See supplement 5 BTrans.m for the values of the constants.

2.5.3 Enzymatic transesterification

Another catalysis method is to use enzymes to assist the transesterification of lipids to FAME's. Tran *et al* described a process in which a lipase enzyme is used to catalyse transesterification (Tran *et al*, 2012). The conversion yield was determined at different ratios between methanol and lipids. A parabolic function was fitted to these data to produce an equation for this relationship.

$$Y = -0.0063 * r^2 + 1.3919 * r + 27.594$$ Eq. 2.47

Where Y is the lipid yield (kg kg^{-1}) and r is the molar ratio between methanol and lipids (kg m^{-3}).

2.6 Combined processes

A number of studies have been done to integrate various process steps. The goal is to reduce the energy consumption. These process consume a considerable amounts of energy, they encompass multiple process steps. Whole algae cells are converted to FAME's. There are three mass balances describing this process:

$$0 = F_L * C_{L,in} - F_L * C_{L,out} - L$$ Eq. 2.48

$$0 = L - F_L * C_{F,out}$$ Eq. 2.49

$$0 = F_{M,in} - F_{M,out} - M$$ Eq. 2.50

$$C_{L,in} = C_{A,in} * AOC$$ Eq. 2.51

$$L = F_L * C_{L,in} * Y$$ Eq. 2.52

$$C_{F,out} = \frac{L}{F_L}$$ Eq. 2.53

$$C_{L,out} = \frac{F_A * C_{L,in} - L}{F_L}$$ Eq. 2.54

$$M = 3 * \frac{L}{m_L} * m_M * \frac{1}{\rho_M}$$ Eq. 2.55

$$F_{M,out} = F_{M,in} - M$$ Eq. 2.56

Where F is the volumetric flow rate (m^3 s^{-1}), C is the concentration (kg m^{-3}), L is the lipid transfer (kg s^{-1}), M is the methanol consumption (kg s^{-1}), m is the molecular weight (kg mol^{-1}) AOC is the algal oil content (%), and ρ is the density (kg m^{-3}). The subscripts L, F and M are lipid, FAME and methanol respectively.

The energy balance is described by:

$$0 = c_{p,A} * F_A * \rho_A * T_{A,in} + c_{p,M} * F_M * \rho_M * T_{M,in} + H - c_{p,F} * F_{F,out} * \rho_F * T_{out} - c_{p,M} * F_M * \rho_M * T_{out} \quad \text{Eq. 2.57}$$

Where c_p is the heat capacity (J kg^{-1} K^{-1}), T is the temperature (K) and H is the power consumption (J s^{-1}).

2.6.1 Supercritical methanol conversion

The supercritical methanol extraction and conversion replaces the disruption, extraction and conversion in a regular process. Methanol is added to the algae slurry. Then the mixture is brought to supercritical conditions. These harsh conditions destroys the cells. The methanol is used as a solvent and it is also use for the transesterification.

Patil *et al* described the relationship between the FAME yield and the temperature (°C) the ratio between algae and methanol (wt/vol) and the reaction time.

$$Y = a0 + a1 * T + b1 * r + c1 * t + a2 * T^2 + b2 * r^2 + C2 * t^2 + ab * T * r + ac * T * t + bc * r * t \quad \text{Eq. 2.58}$$

Where Y is the FAME yield (%), T is the temperature (°C), r is the ratio between methanol and algae (vol/wt) and t is the reaction time (h). See supplment 6 SCM.m for the values of the constants.

2.6.2 Microwave assisted conversion

The microwave assisted conversion replaces the disruption, extraction and conversion steps. The microwaves disrupt the cells. The methanol acts a solvent and reactant. Patil *et al* described the relationship between the FAME yield and the power consumption (W), the reaction time (s) and the algae concentration (%).

$$Y = a0 + a1 * H + b1 * t + c1 * C_{A,in} + a2 * H^2 + ab * H * t + ac * H * C_{A,in} + b2 * t^2 + bc * t * C_{A,in} + c2 * C_{A,in}^2 \quad \text{Eq. 2.59}$$

Where Y is the FAME yield (kg kg^{-1}), H is the power consumption, t is the reaction time (min), and C_A is the algae concentration (kg m^{-3}). See supplement 7 MWEx.m for the values of the constants.

2.7 Pumping

The algae slurry has to be pumped from one unit operation to the next. Since the number of operations in each process chain can be varied. The energy requirement for the pumping of the slurry has to be taken into consideration.

The energy consumption for pumping of the algae slurry between processes has been described by Wileman *et al* as a function of the process parameters. It is assumed that the flow is laminar, because the pipe is wide and the speed is low.

$$H = 2 * f * \rho_A * \frac{F_A^3 * L}{A * D} \quad \text{Eq. 2.60}$$

$$f = \frac{16}{Re} \quad \text{Eq. 2.61}$$

Where H is the power consumption (J s^{-1}), f is the Fanning friction factor, ρ is the density (kg m^{-3}), F is the volumetric flow rate (m^{-3} s^{-1}), L is the length of the tube (m), A is the cross-sectional area (m^2), d is the diameter of the tube (m) and Re is the Reynolds number.
For a laminar flow regime the Reynolds number is given by:

$$Re = \frac{\rho_a * u^{2-n} * D^n}{8^{n-1} * K} \quad \text{Eq. 2.62}$$

Where u is the flow speed (m s^{-1}), K is the consistency factor (Poise/m) and n is the behaviour index. K and n depend on the biomass concentration.

3. Optimization procedure

The goal of this project is to find the best combination of unit operations for the production of biodiesel from microalgae. In chapter 2 all the models, which describe these processes, have been explained. In this chapter the optimization procedure will be described. In the first part a procedure is described, where the values for all process parameters are kept constant at values as reported in literature (refer to literature). This is done through binary optimization. These constant conditions make the procedure relatively simple, since the number of possibilities is kept low. A number of papers have discussed similar methodologies, such a combinatorial approach. In the second optimization the process parameters will be variable within certain bounds. This increases the complexity and computational time of the routine, but it also supplies extra information.

3.1 Binary simulations

For the binary simulations the process conditions are kept constant. Therefore a constant value can be calculated for the energy requirement of each unit operation. This value is multiplied by a binary variable. This variable can have the value 0 or 1. If it is 1 the unit operation is used in the process chain. If it is 0 it is not used. To obtain the total energy requirement the product of the energy requirement and the binary variable for each unit operation is summed.

$$H_{Tot} = \sum_{i=1}^{21} H_i * x_i \qquad \text{Eq. 3.1}$$

Where H is the power requirement (J s^{-1}), x is the binary variable and the index i denotes the different unit operations.

The following optimization is then carried out.

$$Given\ equation\ 2.1 - 2.63 \qquad \text{Eq. 3.2}$$
$$\min Htot(x1 - x21) \qquad \text{Eq. 3.3}$$
$$x1 - x21 = 0|1$$

To make sure that all processes are physically possible, a number of constraints have to be applied to the system. For each unit step only one unit operation can be chosen.

$$x_1 + x_2 + x_3 + x_4 + x_5 + x_6 = 1 \quad \text{Eq. 3.4}$$
$$x_7 + x_8 + x_9 + x_{20,a} = 1 \quad \text{Eq. 3.5}$$
$$x_{10} + x_{20,b}x_{21,a} = 1 \quad \text{Eq. 3.6}$$
$$x_{11} + x_{12} + x_{13} + x_{20,c} + x_{21,b} = 1 \quad \text{Eq. 3.7}$$
$$x_{14} + x_{15} + x_{16} + x_{20,d} + x_{21,c} = 1 \quad \text{Eq. 3.8}$$
$$x_{17} + x_{18} + x_{19} + x_{20,e} + x_{21,d} = 1 \quad \text{Eq. 3.9}$$

Two extra constraints have to be included to govern the combined processes.

$$x_{20,a} = x_{20,b} = x_{20,c} = x_{20,d} = x_{20,e} \quad \text{Eq. 3.10}$$
$$x_{21,a} = x_{21,b} = x_{21,c} = x_{21,d} \quad \text{Eq. 3.11}$$

Where x_1=centrifugation, x_2=pressure filtration, x_3=vacuum filtration, x_4=ultra-sound sedimentation, x_5=chitosan flocculation, x_6=poly-glutamate flocculation, x_7=centrifugation, x_8=pressure filtration, x_9=vacuum filtration, x_{10}=dryer, x_{11} =bead milling, x_{12}=high pressure homogenization, x_{13}=sulfuric acid treatment, x_{14}=hexane extraction, x_{15}=mixed solvent extraction, x_{16}=$SCCO_2$ extraction, x_{17}=acid catalysed conversion, x_{18}=base catalysed conversion, x_{19}=enzymatic conversion, x_{20}=SCMeOH conversion, x_{21}=microwave assisted conversion. See supplement 8 BIntRun.m for the full routine.

It would also have been possible to use a different approach for these calculations using the binary integer programming function of Matlab. The main disadvantage of this procedure is that it gives only one (the best) solution. Thus leaving out a lot of information about the system and other possibilities that might be almost as good.

3.2 Mixed integer optimization

As mentioned in the introduction section 1.2, the mixed integer non-linear optimization is used to evaluate a system that is more flexible than that of the binary simulations. The operating conditions for each process for binary simulations and the range of conditions for the mixed integer optimization are given in appendix C. To illustrate the potential of a flexible optimization an example is considered. In the binary optimization there is a process route that uses centrifugation for successively harvesting and mechanical dewatering. These steps consume a lot of energy. The total concentration factor over both steps is 40. This concentration factor is obtained by 10 times during concentration during harvesting and 4 times during dewatering. But also other combinations of concentration during harvesting and dewatering are possible. The energy consumption for a range of possible combinations is given in in figure 3.1.

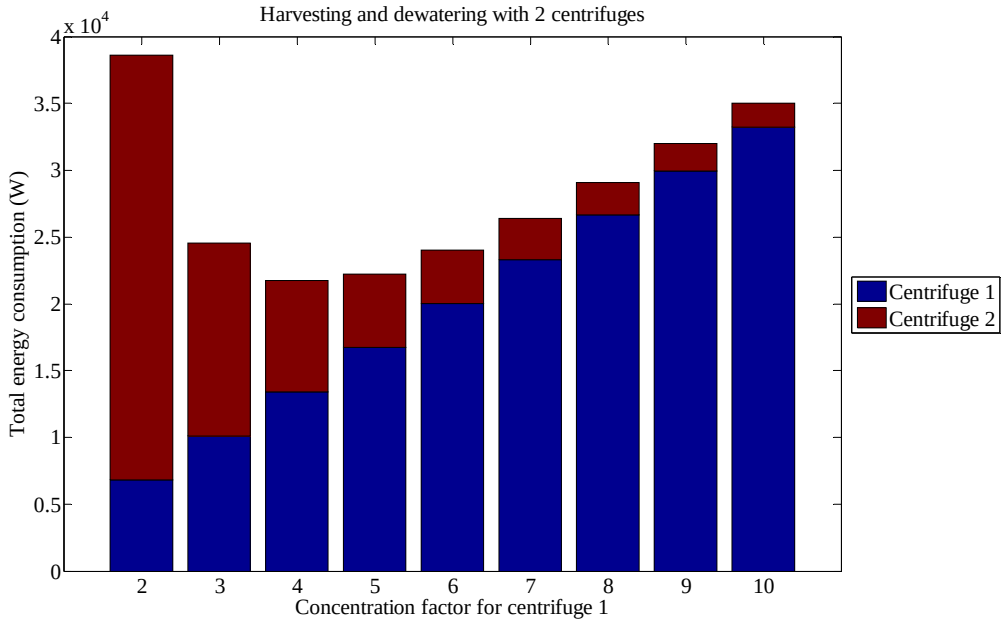

Fig. 3.1 - Energy requirement for a system where centrifugation is used for harvesting and mechanical dewatering. Blue shows the contribution of harvesting to the total energy requirement and red the contribution of mechanical dewatering.

Figur 3.1 shows that the best solution is obtained by 4-5 times concentration in harvesting and subsequently 10-8 times concentration during dewatering . This is shown by bars 3 and 4. The example shows that the energy consumption can be reduced by a further optimization of processing parameters.

A combined optimization for product routing and process parameters is a mixed integer non-linear optimization (MINLP). The problem is defined as:

$$Given\ equation\ 2.1 - 2.63 \quad \text{Eq. 3.12}$$
$$\min Htot(\text{x1-x21}) \quad \text{Eq. 3.13}$$
$$x1 - x21 = 0|1$$

The difference with the binary simulations lies in the variable operating conditions (see appendix C). The mixed integer non-linear optimization was carried out using Tomlab. The same constraints applied as for the binary simulations. There are also extra constraints on the decision variables. These are given in table B.1 (see appendix B). See supplement 9 MINLP for the full routine.

4. Results and discussion

Two methods to evaluate the best route for biodiesel production have been considered, binary simulations and mixed integer optimization. In the binary simulations all process parameters are kept constant, while with the mixed integer optimization process parameters are optimized in combination with the product routing.

4.1 Binary simulations

For the binary simulations all combinations of the available unit operations were evaluated for their total energy requirement and the contribution of each step to the total at fixed process conditions. The process starts with a biomass concentration of 5 kg m^{-3}. It is harvested resulting in a biomass concentration of 50 kg m^{-3} with a recovery of 95% of the algae. Mechanical dewatering is used to concentrate the slurry to 200 kg m^{-3} with a recovery of 95% of the algae biomass. Drying increases the biomass concentration to 800 kg m^{-3} with no loss of algal biomass. Disruption destroys 90% of the algae cells. Using extraction 95% of the lipids are recovered. Finally, transesterification converts 95% of the lipids to biodiesel.

Table 4.1 – Changes during the different process steps for the binary simulations.

Process step	Change	Value
Harvesting	Concentration factor	10
	Microalgae recovery	95%
Mechanical dewatering	Concentration factor	4
	Microalgae recovery	95%
Thermal dewatering	Concentration factor	4
	Microalgae recovery	100%
Disruption	Disruption yield	90%
Extraction	Extraction yield	95%
Transesterification	Yield	95%
Combined processes	Yield	75%

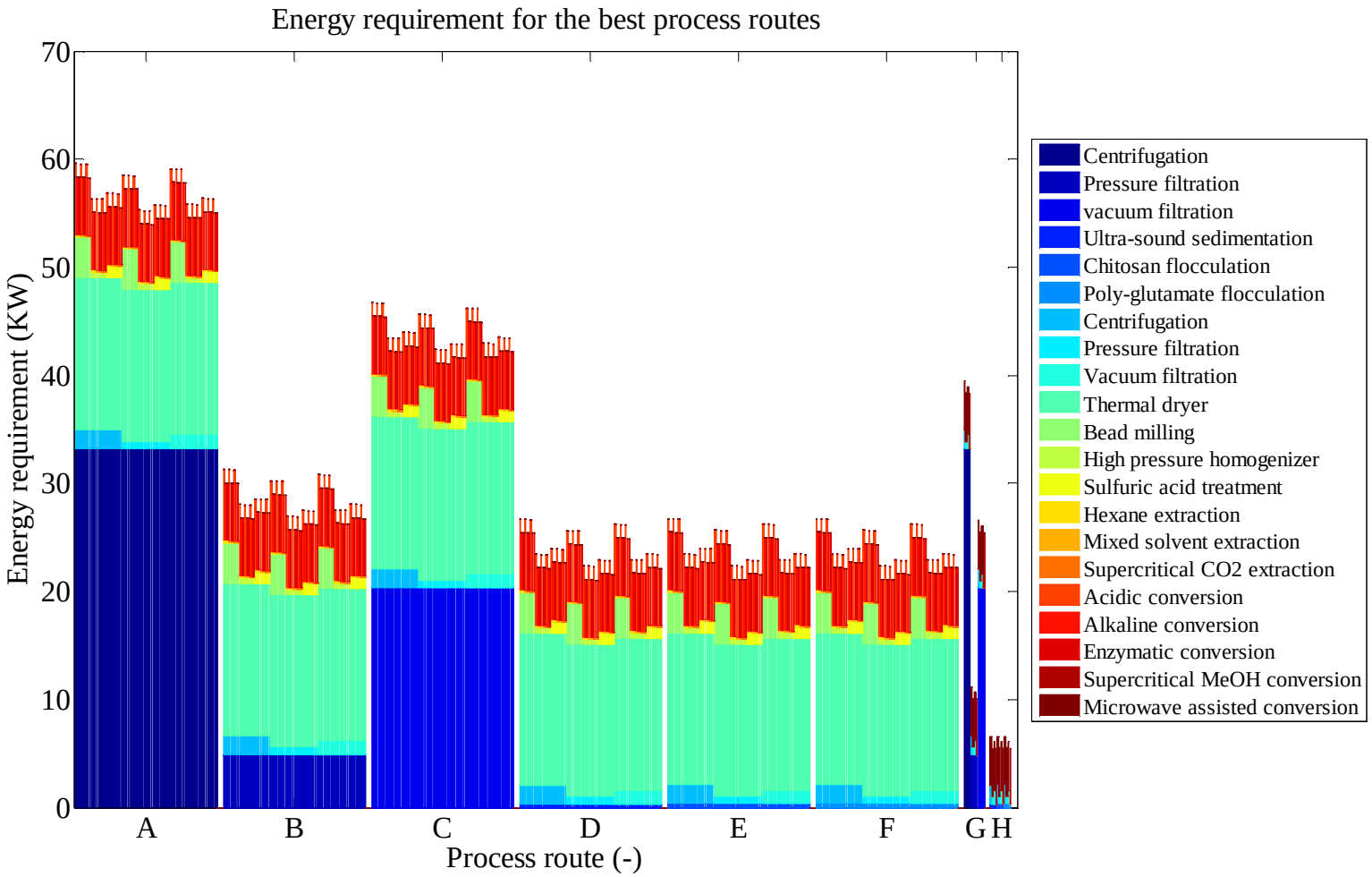

Fig. 4.1 – Binary optimization runs for the production of biodiesel. Each bar contains the cumulative energy requirement for each process route. On the x-axis the groups of process routes are denoted. The y-axis displays the energy requirement in KW.

Figure 4.1 shows the energy requirement for each process chain. It is built by stacking the energy requirement for each process step. A number of trends can be deduced from this graph. Group A includes all process routes, in which centrifugation is used for harvesting. For group B all processes are harvested using pressure filtration. For group C this is done by vacuum filtration. In group D ultra-sound sedimentation is used for harvesting. In group E the algae are harvested using chitosan flocculation. For group F the algae are harvested using poly-glutamate flocculation. Group G and H use supercritical methanol conversion or microwave assisted conversion to turn wet algae into biodiesel. In group G algae are harvested using centrifugation, pressure filtration or vacuum filtration and in group H by ultra-sound sedimentation, chitosan flocculation or poly-glutamate flocculation.

The first trend that can be seen is that the conventional harvesting process (group A, B and C) take more energy compared to the innovative separation methods (group D, E and F). This is caused by the large flows that needs to be processed. Ultra-sound sedimentation, chitosan flocculation and poly-glutamate flocculation have to process the same volumetric flow, but they only require energy for creating a standing wave or mixing the flocculant with the algae. The actual removal and concentration is done by gravity.

In the mechanical dewatering step centrifugation, pressure filtration and vacuum filtration are used in all process routes to concentrate the algae slurry further. Because these processes are also used for harvesting, it might be expected that the energy requirement for these steps would be in the same order of magnitude. This is not the case. The difference in energy requirement between the harvesting and the mechanical dewatering can be explained by two factors. First the concentration factor dewater the algae is smaller than for harvesting. For the harvesting the fermentation broth is concentrated 10 times, while the flow is reduced only four times during the mechanical dewatering. Second the volumetric flow that has to be processed is almost 10 times smaller after the harvesting. This results in a 7-fold reduction of energy The data from the simulations also supports this. The energy required for harvesting using centrifugation is 33168 W and for mechanical dewatering using centrifugation it is 1662 W.

Thermal dewatering is also a step that consumes a significant amount of energy. This is the third step in all process chains in group A to F. This is at least partly caused by the value that is assumed for the efficiency of the thermal dryer (50%). To reduce the energy consumption

part of the energy is recovered after drying using a single heat exchanger. This also holds for every other unit operation where the reaction temperature is higher than 50° C. Using more complex systems of heat exchangers the efficiency might be increased to 80%-90%. This will make the system far more complex, which increases the time required for the calculations.

The last step which has a noticeable contribution to the total energy requirement is the disruption step. This is caused by the use of physical forces to disrupt cells. Here part of the energy is lost due to the incomplete transfer of the energy from the machinery to the algae.

During the harvesting and dewatering processes the algae broth has become quite viscous. This increases the energy that is required for pumping. The energy required for pumping has increased about 10 fold. Therefore processes that need a high biomass concentration need more energy for pumping.

The low energy use in the extraction and conversion step is caused by the very low volumetric flow rate compared to the earlier steps. During harvesting 1 m^3 h^{-1} has to be processed. During extraction and conversion about 0.005 m^3 h^{-1} has to be processed.

There are 24 routes (groups G and H) that have not been considered yet. These routes include combined extraction and conversion steps. These conversions steps can be combined with conventional (group G) or innovative (group H) harvesting steps. As before the conventional harvesting steps increase the energy requirement dramatically compared to the innovative harvesting steps. The supercritical methanol extraction and conversion, is a large contributor to the overall energy requirement of the route. This is due to the rather large volumetric flow that has to be processed, about 0.1 m^3 h^{-1} and the supercritical conditions of at least 250° C and 60 bars.

The best processes involve the microwave assisted conversion of the microalgae to biomass. The water content does not have to be very low, and thermal drying is not required. Furthermore the conditions at which the reaction takes place are mild (60° C). This leads to a difference of energy requirement between these cases and the worst cases of at least 7 times. The best processes are illustrated in detail in figure 4.2.

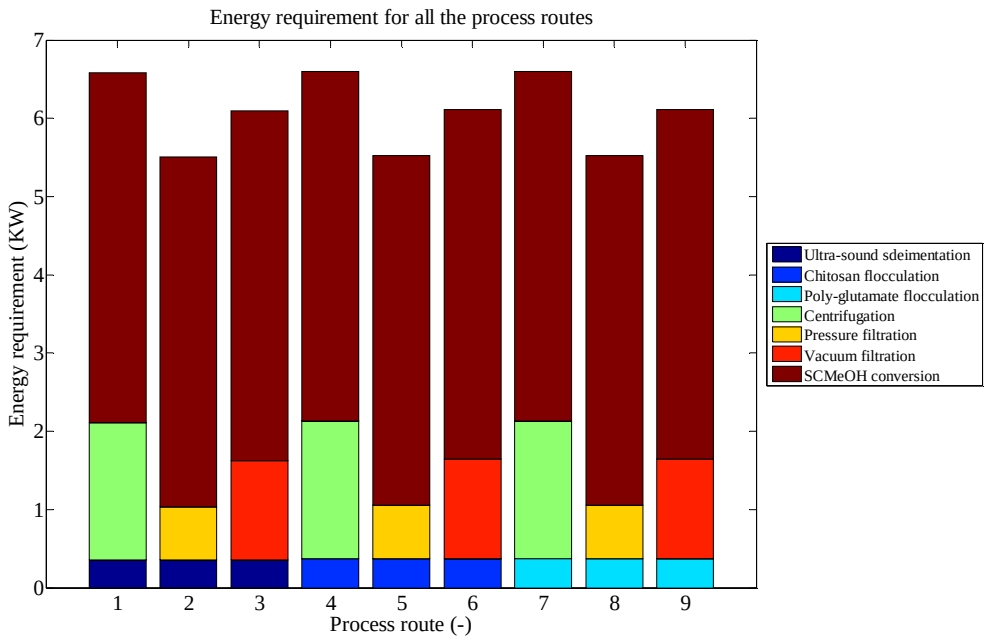

Fig. 4.2 – Energy requirement of the best processes for the production of biodiesel. The bars represent the cumulative energy requirement for each process route. On the x-axis the number of each route is displayed. On the y-axis the energy requirement is displayed in KW.

For the best cases, the conversion step has the major share in the energy consumption (dark red). This process takes up more than 6 KW of the total energy required. In comparison harvesting takes up about 250 W and dewatering takes from 400 to 1700 W. The biggest difference in energy requirement is caused by the mechanical dewatering step. When pressure filtration is used, the energy requirement is lowest. The harvesting step (dark to light blue) has a small difference on the overall energy consumption; therefore we have to look at the other process parameters to find the best option. This will give us other possibilities to improve the choice of the final process route.

The energy requirement, the number of unit operations, the material use and the process conditions are given in a spiderplot, see figure 4.3.

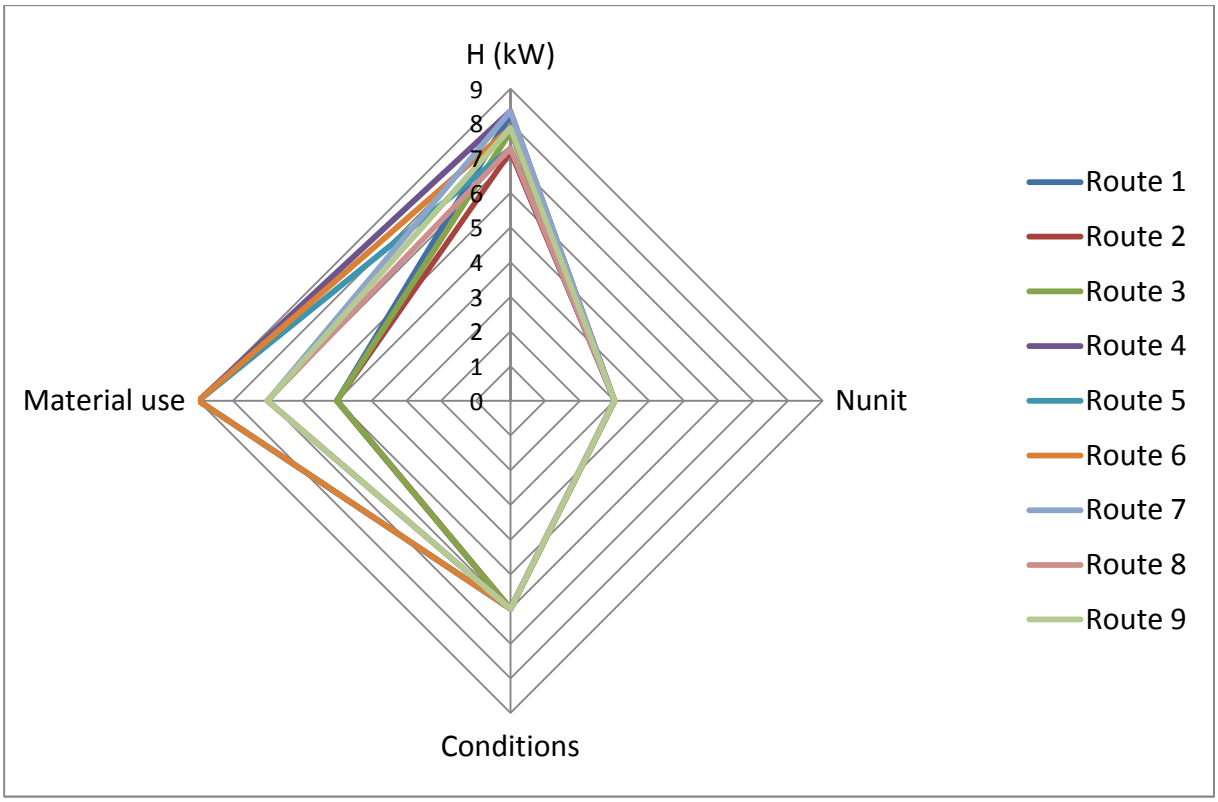

Fig. 4.3 – Different considerations to find the best case for the production of biodiesel. *H* is the energy requirement in KW, N_{unit} is the number of unit operations, conditions represent the process conditions (mild vs harsh) and material use represents the material use. The operating conditions and material use are qualitative variables. The operating conditions increases 1 for every 10° C above room temperature and 2 for every bar above ambient pressure. The material use increases 1 for every 15 mg L^{-1} of flocculant and 1 for every 0.1 m^3 of methanol.

The best route amongst the routes given in figure 4.2 is harvesting by ultra-sound sedimentation, followed by pressure filtration, followed by microwave assisted conversion (number 2 in figure 4.2). It has the lowest energy consumption and material use. Processes, where the ultrasound sedimentation is replaced by a flocculation, are also very good (number 5 and 8 in figure 4.2). These only have a small increase in energy requirements and they both use a flocculant.

4.1.1 Relative contribution of each processing step

To evaluate the contribution of each process step to the total energy requirement of a process route, the energy requirement for that step was divided by the total energy requirement. This is done for one route of each group denoted in figure 4.1. The results are displayed in figure 4.4.

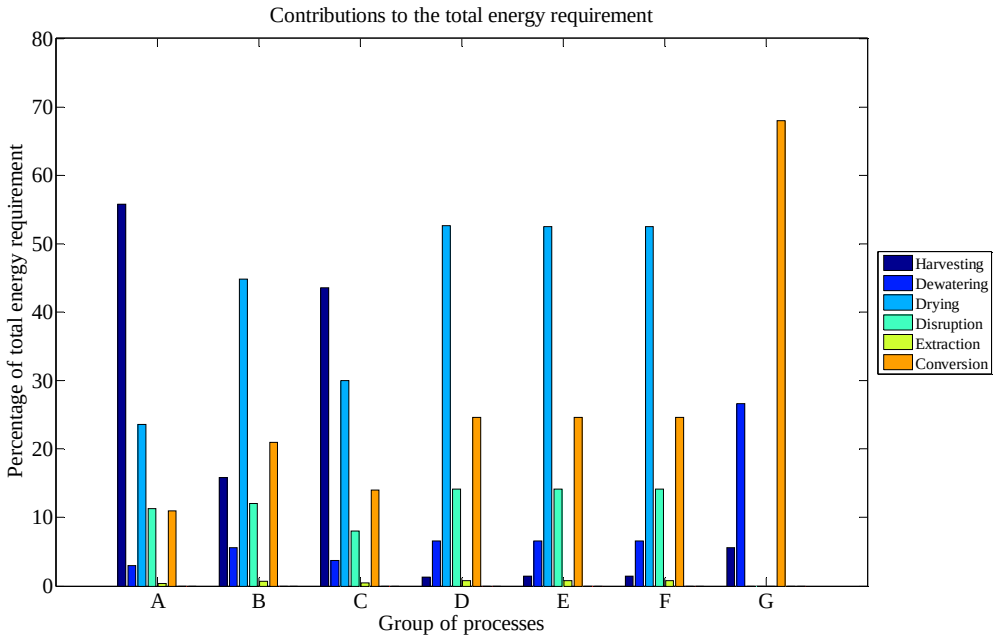

Fig. 4.4 – Contribution of each process step to the total energy requirement of a process route for different groups of processes. The x-axis denotes the different process groups. They are the same groups as in figure 4.1. The y-axis displays the percentage of the total energy requirement.

Since the harvesting step generates the greatest difference in total energy requirement, the processes were grouped on their harvesting process as with figure 4.1. The first group uses centrifugation for harvesting, the second group pressure filtration, the third vacuum filtration, the fourth ultra-sound sedimentation, the fifth chitosan flocculation, the sixth poly-glutamate flocculation and the seventh groups uses combined step for disruption, extraction and conversion. For each group of processes the route with the highest total energy requirement was used. When centrifugation is used for harvesting, at least 70% of the total energy requirement is caused by this step. For the vacuum filtration is used this is at least 60%. With these two groups of processes the other process steps only have minor contributions to the

overall energy requirement. To reduce the energy demand the focus should be on reduction in these steps.

In cases where pressure filtration is used, the biggest contributor is the drying process, followed closely by the harvesting and disruption step. At the moment one heat exchanger is used to recover energy during heating. When a more complex system of heat exchangers is used this contribution can be lowered.

In groups D, E and F ultra-sound sedimentation, chitosan flocculation and poly-glutamate flocculation are used respectively. With these routes the energy demand for harvesting is very low, therefore other process steps gain a larger contribution to the total. In all these processes the drying step is the biggest contributor.

The last group of processes use a combined disruption, extraction and conversion step to convert wet algae to biodiesel. This omits the need for drying. The biggest contributor is the combined step.

4.1.2 Comparison with literature

To evaluate the results of this project, they are compared to data from papers from Delrue *et al* and Brentner *et al* (Delrue *et al*, 2012; Brentner *et al*, 2011). To this end data were converted to net-energy return (NER) values. The value describes the amount of energy that is produced in the form of biodiesel for the energy that is used for downstream processing, which is calculated from the power requirement, energy requirement and the specific energy requirement.

$$NER = \frac{P_{biodiesel}}{P_{downstream}} = \frac{E_{biodiesel}}{E_{downstream}} = \frac{e_{biodiesel}}{e_{downstream}} \qquad \text{Eq. 4.1}$$

Where *NER* is the net-energy return (-), *P* is the power requirement (J s^{-1}), *E* is the energy requirement (J) and *e* is the specific energy requirement (J kg^{-1}).

This calculation was performed for each group of processes from this project; the best en most conservative case from Brentner *et al* and the best and most conservative cases of Delrue *et al* (Brentner *et al*, 2011)(Delrue *et al*, 2012).The results are shown in figure 4.5.

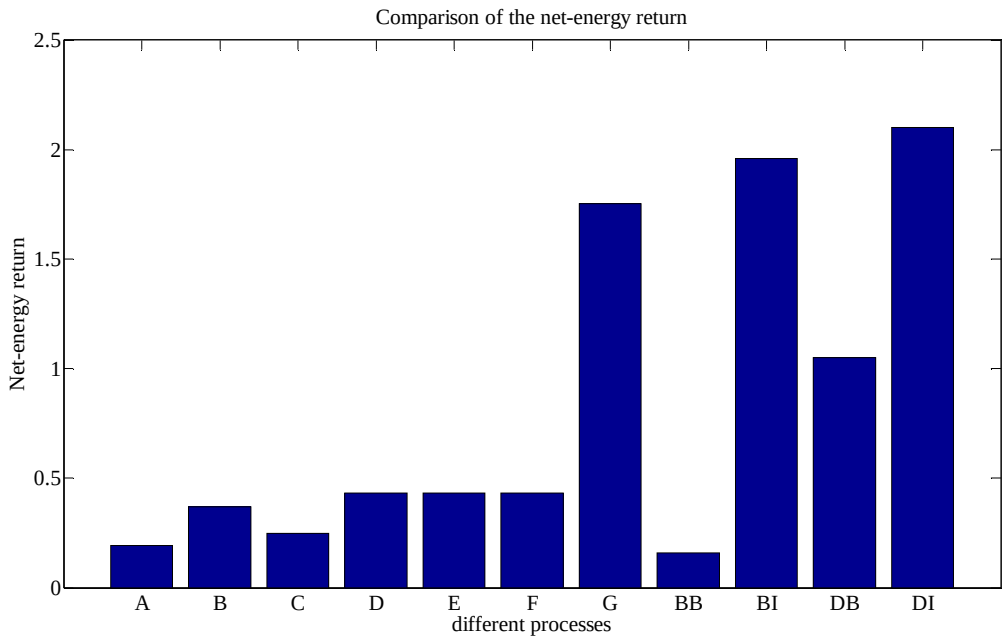

Fig. 4.5 – Comparison of the NER between the results of this project and data from literature. The x-axis shows the different process routes. A to G represent the same groups as in figure 4.1; BB and BI are the base and innovative case from Brentner *et al* and DB and DI are the base and innovative cases from Delrue *et al*.

In figure 4.5 the first seven bars depict the results from this project, bar BB and BI depict results from Brentner *et al* and bar DB and DI depict the results from Delrue *et al*. Bars A, BB and DB depict base cases, where more conventional methods are used for the production of biodiesel. The results of this project are comparable with those from Brentner *et al*. The base case of Delrue *et al* differs in the unit operations that were used for harvesting.
Bar G, BI and DI depict the most innovative cases. These routes use wet algae to remove the necessity of extra drying. Only the innovative cases of this project, Brentner *et al*, Delrue *et al* and the base case of Delrue *et al* have a net energy-return higher than 1. Therefore only these processes produce more energy than they consume.

There are different ways to model each unit operation. In this project mass and energy balances are used to create the models. Brentner *et al* used constants from literature to describe processes under certain conditions. Delrue *et al* uses an approach similar to uncertainty analysis, where the result of the calculations is a range in which 50% of the solutions lie. This causes a difference in the results, because different assumptions are made.

One of the causes of the differences is the energy that is required for pumping. This project uses a model from Wileman *et al* to describe the energy requirement for pumping. In this model the pumping energy depends on concentration and flow rate, both Brentner and Delrue have used constant values or a range of values for the energy required for pumping.

4.2 Mixed integer optimization

While an approach with constant process parameters gives a good result. It is interesting to find out if an optimization with flexibility for the process parameters will give a better solution. Therefore Tomlab is used to perform mixed integer non-linear optimization of the same models as are used for the binary simulations. The bounds on the process parameters can be found in Appendix B (see appendix B).

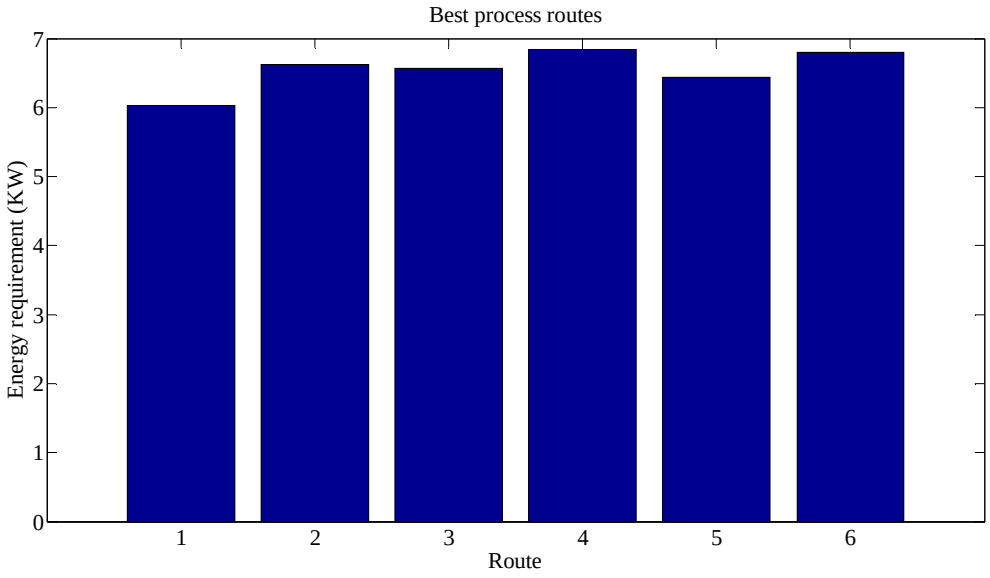

Fig. 4.6 – Energy requirement for the best process routes after MINLP. The bars show the cumulative energy requirement of each route. The x-axis shows the number of the process route. The y-axis displays the energy requirement in KW

As with the binary optimization the best solutions include a novel harvesting step combined with microwave assisted extraction. For dewatering they either use pressure or vacuum filtration. The best process takes a little more than 6000 W and the least efficient of these takes about 7000 W. About 75% of this is caused by the microwave assisted conversion. 5% is caused by harvesting and 20 % is caused by dewatering.

To consider the improvement after mixed integer optimization to the binary simulations the net-energy return of the mixed integer optimization was divided by the net-energy return of the binary simulations for seven process routes. This results in a percentage of the original energy requirement.

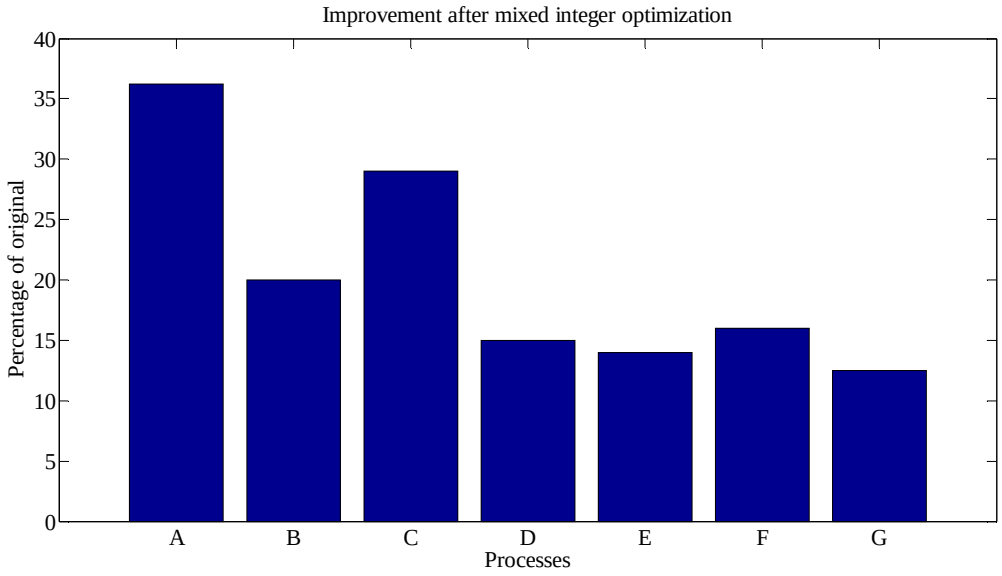

Fig. 4.7 – Comparison of energy requirement after mixed integer optimization to after binary optimization. The bars represent the reduction of the total energy requirement after MINLP compared to the binary simulations. The x-axis shows the group of process routes as in figure 4.1. The y-axis shows the reduction as a percentage of the total energy demand of the binary simulations.

The routes A to G represent centrifugation, pressure filtration, vacuum filtration, ultra-sound sedimentation, chitosan flocculation or poly-glutamate flocculation for harvesting and combined extraction and conversion processes respectively.

The improvement varies between 65 and 90% of the original energy requirement. The best improvements can be gained in the harvesting processes. This is especially the case for the vacuum filtration and the centrifugation steps for harvesting, since these processes are large contributors in their respective routes. There is less improvement in the steps after water removal, because reactions can take place in a smaller range of process parameters, thus limiting the optimization possibilities. The difference in improvement between groups A to G is caused by the level of optimization that was already done in the models. The more innovative are valid in a smaller range therefore the optimization is not very large. The

models for the harvesting and dewatering steps are valid within a large range. Therefore larger improvements can be made here.

5. Conclusion

Production of biodiesel from microalgae is an important solution to cope with the depleting oil reserves, to avoid deforestation and reduce the competition between food and non-food use of agricultural products. The bottleneck in the production of biodiesel from micro algae that is considered in this project is the energy requirement for downstream processing. The goal of this project is to reduce this energy demand.

To this end models are made to describe different unit operations involved in the downstream processing of microalgal biomass to biodiesel. Networks of these models were then evaluated to find the route with the lowest energy requirement. This is done through two different approaches. The first concerned binary simulations in which all possible routes are evaluated, while all process parameters were kept constant. From these results it can be concluded that process chains that do not need extensive drying and that use combined disruption, extraction and conversion steps are the most energy efficient. Here microwave assisted extraction and conversion is preferable to supercritical methanol extraction, because the energy requirement is lower and because the operating conditions for SCM processes are rather extreme. Among the best solutions the differences in energy requirement are very small. The decision thus hinges on the other considerations. When ultrasound sedimentation is used there are no material demands for harvesting. For all the best routes the number of used unit operations is three. The operating conditions are also the same. Therefore it is concluded that the best route consists of ultra-sound sedimentation, pressure filtration and microwave assisted conversion. Beside the lowest energy demands it has the lowest use additional resources. The most energy inefficient processes use centrifugation or vacuum filtration plus extensive drying to remove water from the algae.

The second approach uses mixed integer non-linear programming to minimize the energy demand. For these processes the process parameters are also optimized within bounds. This gave extra flexibility to the models during optimization, which lead to better solutions. The best and worst solutions for this approach are the same kind of routes as the binary optimization. There is a difference in the improvement between these approaches. For example in the chain of unit operations that use vacuum filtration and centrifugation the energy demand can be reduced to 65 to 75% of the energy demand obtained from the binary

simulations. For the other processes the energy requirement lies between 80 and 90% of the energy demand obtained from the binary simulations.

Reduction in the flow rate has a positive effect on the energy demand at first, since the volumetric flow rate that needs to be processed decreases. When the algae slurry is very concentrated the energy demand for pumping starts to increase. Therefore wet processes are preferable.

This work is uses basic mass and energy balances. The result of the calculations can be improved further by increasing the amount of detail of the models and by doing more research into wet algae processes and novel harvesting methods.

Finally it is concluded that using an optimization method to determine the total energy demand can give considerable improvement to a method where process parameters are kept constant. In the best cases energy requirement is reduced between 30 to 40%. With this information future studies can improve their results drastically.

References

Amaro, H. M., A. C. Guedes, et al. (2011). "Advances and perspectives in using microalgae to produce biodiesel." Applied Energy 88: 3402-3410.

Best practice manual – Dryers, Devki Energy Consultancy Pvt. Ltd., 405, Ivory Terrace, R.C. Dutt Road, Vadodara – 390007, India.

Bosma, R., W. A. van Spronsen, et al. (2003). "Ultrasound, a new separation technique to harvest microalgae." Journal of applied phycology 15(2): 143-153.

Brentner, L. B., M. J. Eckelman, et al. (2011). "Combinatorial Life Cycle Assessment to Inform Process Design of Industrial Production of Algal Biodiesel." Environmental Science & Technology 45: 7060-7067.

Char J., J. Wang, et al. (2011), "Biodiesel production form microalgae through supercritical carbon dioxide extraction", Journal of the Japan Insitute of Energy 90: 369-373.

Demirbas, A. and M. Fatih Demirbas, Algae Energy: Algae as a new source of biodiesel, Springer 2010.

Delrue, A., P.-A. Setier, et al. (2012), "An economic, sustainability, and energetic model of biodiesel production from microalgae", Bioresource Technology 111: 191-200

Doucha, J. and K. Lívanský (2008). "Influence of processing parameters on disintegration of Chlorella cells in various types of homogenizers." Applied Microbiology and Biotechnology 81: 431-440.

Halim, R., R. Harun, et al. (2011). "Microalgal cell disruption for biofuel development." Applied Energy 91: 116-121.

Morales, J., J. de la Noüe, et al. (1985). "Harvesting marine microalgae species by chitosan flocculation." Aquacultural Engineering 4: 257-270.

Patil, P. D., V. Gnaneswar Gude, et al. (2011), “Optimization of direct conversion of wet algae to biodiesel under supercritical methanol conditions”, Bioresource Technology 102 (2011) 118–122.

Patil, P. D., V. Gnaneswar Gude, et al. (2011), “Optimization of microwave-assisted transesterification of dry algal biomass using response surface methodology”, Bioresource Technology 102: 1399-1405.

Sialve, B., N. Bernet, et al. (2009). "Anaerobic digestion of microalgae as a necessary step to make microalgal biodiesel sustainable." Biotechnology advances 27: 409-416.

Stephens, E., I. L. Ross, et al. (2010). "Future prospects of microalgal biofuel production systems." Trends in plant science 15: 554-564.

Tenney, M. W., W. F. Echelberger, et al. (1969). "Algal Flocculation with Synthetic Organic Polyelectrolytes." Applied Microbiology 18: 965-971.

Tran, D., K. Yeh, et al. (2012), “Enzymatic transesterification of microalgal oil from Chlorella vulgaris ESP-31 for biodiesel synthesis using immobilized Burkholderia lipase”, Bioresource Technology 108: 119–127.

Rashid, U., F. Anwar, et al. (2009), “Optimization of alkaline transesterification of rice bran oil for biodiesel production using response surfacemethodology”, J Chem Technol Biotechnol 84: 1364–1370.

Venkata Mohan, S., M. Prathima Devi, et al. (2011). "Potential of mixed microalgae to harness biodiesel from ecological water-bodies with simultaneous treatment." Bioresource technology 102: 1109-1117.

Wileman, A., A. Ozkan, et al. (2012). "Rheological properties of algae slurries for minimizing harvesting energy requirements in biofuel production." Bioresource technology 104: 432-439.

Zheng, H., Z. Gao, et al. (2012). "Harvesting of microalgae by flocculation with poly (γ-glutamic acid)." Bioresource technology 112: 212-220.

Appendix – Example of a model

```
function [ C , D , H ] = Cent( A , Cf )
%   Cent describes a centrifuge
%   Given the properties of an algae flow and a concentration factor as
inputs,
%   this function will calculate a concentrated algae flow a waste flow
%   and the power consumption.
%   A C and D are of the form A = [ F , C1 , C2 , T  , p ]
%   The concentration factor and the power consumption are both scalars

% Disassembly
AF = A(1);                                  % Volumetric flow rate (m^3 h^-1)
AC1 = A(2);                                 % Biomass concentration (kg m^-3)
AC2 = A(3);                                 % Not applicable
AT = A(4);                                  % Temperature (K)
Ap = A(5);                                  % Pressure (bar)

% Mass balances
R = 0.95;                                   % Microalgae recovery (kg kg^-1)
CC1 = AC1 * Cf;                             % Biomass concentration (kg m^-3)
CF = AF * AC1 * R / CC1;                    % Volumetric flow rate (m^3 h^-1)
CC2 = AC2;                                  % Not applicable
DF = AF - CF;                               % volumetric flow rate (m^3 h^-1)
DC1 = AF * AC1 * ( 1 - R ) / DF;            % Biomass concentration (kg m^-3)
DC2 = AC2;                                  % Not applicable

% Energy Balances
CT = AT;                                    % Temperature (K)
Cp = Ap;                                    % Pressure (bar)
DT = AT;                                    % Temperature (K)
Dp = Ap;                                    % Pressure (bar)
Hh = 0;                                     % Power requirement for heating
and cooling (J s^-1)
E = 11880000;                               % Energy constant (J m^-3)
[Wileman et al]
Hs = E * AF * Cf / 3600;                    % Power requirement for separation
(J s^-1) [Wileman et al]
L = 25;                                     % Pumping distance (m)
Hp1 = pump( CF , CC1 , L );                 % Power requirement for pumping
product (J s^-1)
Hp2 = pump( DF , DC1 , L );                 % Power requirement for pumping
waste (J s^-1)
Hp = Hp1 + Hp2;                             % Total power requirement for
pumping (J s^-1)
H = Hh + Hs + Hp;                           % Total power requirement (J s^-1)

% Assembly
C = [ CF , CC1 , CC2 , CT , Cp ];
D = [ DF , DC1 , DC2 , DT , Dp ];
end
```

Appendix B – Optimization condition

Process	Variable	Binary simulations	MINLP lower bound	MINLP upper bound
Harvesting				
Centrifugation	Temperature (K)	293	293	293
	Pressure (bar)	1	1	1
	Concentration factor	10	1	40
Pressure filtration	temperature (K)	293	293	293
	Pressure (bar)	1	1	1
	Concentration factor	10	1	40
Vacuum filtration	temperature (K)	293	293	293
	Pressure (bar)	1	1	1
	Concentration factor	10	1	40
Ultra-sound sedimentation	Temperature (K)	293	293	293
	Pressure (bar)	1	1	1
	Concentration factor	10	1	20
Chitosan flocculation	Temperature (K)	293	293	293
	Pressure (bar)	1	1	1
	Concentration factor	10	10	10
	Flocculant concentration (g m^{-3})	60	10	100
Poly-glutamate flocculation	Temperature (K)	293	293	293
	Pressure (bar)	1	1	1
	Concentration factor	10	10	10
	Flocculant concentration (g m^{-3})	30	10	60
Mechanical dewatering				
Centrifugation	Temperature (K)	293	293	293
	Pressure (bar)	1	1	1
	Concentration factor	4	1	40
Pressure filtration	temperature (K)	293	293	293
	Pressure (bar)	1	1	1
	Concentration factor	4	1	40
Vacuum filtration	temperature (K)	293	293	293
	Pressure (bar)	1	1	1
	Concentration factor	4	1	40
Thermal dewatering				
Dryer	Temperature (K)	100	100	100
	Pressure (bar)	1	1	1
	Concentration factor	4	4	160

Disruption				
Bead milling	Temperature (K)	293	293	293
	Pressure (bar)	1	1	1
	Bead filling (%)	82	50	90
High pressure homogenizer	Temperature (K)	293	293	293
	Pressure (bar)	850	850	850
Sulfuric acid treatment	Temperature	160	160	160
	Pressure (bar)	1	1	1
Extraction				
Hexane extraction	Temperature	293	293	293
	Pressure (bar)	1	1	1
Mixed solvent extraction	Temperature (K)	323	323	323
	Pressure (bar)	1	1	1
Supercritical CO_2 extraction	Temperature (K)	50	30	70
	Pressure (bar)	225	150	300
Conversion				
Acid catalysed transesterification	Temperature (K)	323	323	323
	Pressure (bar)	1	1	1
	Flow of methanol (m^3 h^{-1})	0.45	0.3	0.9
Base catalysed esterification	Temperature(K)	303	303	303
	Pressure (bar)	1	1	1
	Flow of methanol (m^3 h^{-1})	0.45	0.3	0.9
Enzyme catalysed transesterification	Temperature (K)	333	333	333
	Pressure	1	1	1
	Flow of methanol (m^3 h^{-1})	0.45	0.3	0.9
Supercritical MeOH extraction	Temperature (K)	525	515	535
	Pressure (bar)	80	80	80
	Flow of methanol (m^3 h^{-1})	0.45	0.3	0.9
Microwave assisted conversion	Temperature (K)	333	333	333
	Pressure (bar)	1	1	1
	Flow of methanol (m^3 h^{-1})	0.45	0.3	0.9